Differential Response of Human Lung Epithelial Cells to Particulate Matter in Fresh and Photochemically Aged Biomass-Burning Smoke

Khairallah Atwi[a], Sarah N. Wilson[b], Arnab Mondal[b], R. Clayton Edenfield[c,d], Krista M. Symosko Crow[c,d], Omar El Hajj[a], Charles Perrie[a], Chase K. Glenn[a], Charles A. Easley IV[c,d*], Hitesh Handa[b,e*], Rawad Saleh[a*]

[a]Air Quality and Climate Research Laboratory, School of Environmental, Civil, Agricultural and Mechanical Engineering, University of Georgia, Athens, GA, USA

[b] Handa Biomaterials Research Laboratory, School of Materials, Chemical and Biomedical Engineering, University of Georgia, Athens, GA, USA

[c] Department of Environmental Health Science, College of Public Health; University of Georgia; Athens, GA, USA

[d] Regenerative Bioscience Center; University of Georgia; Athens, GA, USA

[e]Department of Pharmaceutical and Biomedical Sciences; University of Georgia; Athens, GA, USA

[*]*To whom correspondence should be addressed*: rawad@uga.edu, hhanda@uga.edu, cae25@uga.edu.

Abstract

The chemical composition of particulate matter (PM) in biomass-burning smoke evolves upon aging in the atmosphere. The effect of this evolution on the toxicity of biomass-burning PM is understudied. Here, we burned oak foliage, pine needles, and hickory twigs in an environmental chamber. We used UV radiation to initiate photochemical aging of the emissions leading to the production of secondary organic aerosol (SOA), quantified using online particle size distribution measurements, and an overall increase in the PM oxygenation and decrease in the relative abundance of aromatic and condensed aromatic structures, obtained using ultra-high-resolution electrospray ionization mass spectrometry. *In vitro* exposure of human lung epithelial cells to PM from hickory combustion led to the strongest reduction in metabolic activity, followed by pine and oak, which was associated with the heavy metal content of the PM from the three fuels, quantified using induction-coupled plasma mass spectrometry. Furthermore, exposure to the fresh PM led to more reduction in metabolic activity than the aged PM for all fuels, whereas the aged PM induced more cell death by apoptosis. The differential cellular response to the fresh and aged PM indicates that the increase in oxygenation and decrease in aromaticity associated with photochemical aging alters the toxicity mechanisms exhibited by the PM, with a possible role of decreasing the heavy metal content (gram-metals per gram-PM) due to SOA formation. Together, these findings highlight the complex effect of photochemical aging on biomass-burning PM toxicity and motivate further studies to elucidate the underlying differences in toxicity mechanisms between fresh and aged PM.

Keywords: wildland fires, organic aerosol, atmospheric aging, toxicity, apoptosis, mitochondrial dysfunction

1. Introduction

Wildland fires play an essential role in maintaining the health of natural ecosystems[1, 2]. However, they are also major sources of air pollution, with significant impacts on climate[3-6] and public health[7-11]. In 2011, an estimated 212 million people lived in U.S. counties that were affected by wildfire smoke[12]. Further, between 2008 and 2012, more than 10 million people lived in counties that had unhealthy air quality for over ten days a year due to wildfire smoke, with particular implications for vulnerable communities[13]. As the response to air pollution and climate change gears toward lower anthropogenic emissions, and as the increase in global temperatures and drought episodes drives wildland fires to increase in frequency and intensity[14, 15], emissions from wildland fires could become the dominant health risk caused by air pollution for millions of people[16].

Inhalation exposure to particulate matter (PM) emitted from wildland fires has been associated with lung diseases including asthma and chronic obstructive pulmonary disease (COPD)[17-19]. However, understanding of the toxicity mechanisms underlying these health effects is still lacking[3, 10, 19, 20]. Measurements of biological markers from humans exposed to wildland-fire smoke[21, 22], *in vivo* exposure studies[23], and *in vitro* exposure studies[24-26] have revealed various toxicological effects including oxidative stress, inflammation, and cell death by apoptosis/necrosis. Biomass-burning PM is mostly composed of organic aerosol (OA)[27, 28], which includes a myriad of organic species with varying physicochemical properties[26, 29-31]. Hereafter, we use OA when we refer to the organic fraction of the PM, and PM when we refer to the overall particulate matter, which, in addition to OA, includes elemental carbon, inorganic salts, and metals[27, 32]. Different OA components can induce different toxicity mechanisms. Pardo et al.[33] exposed lung epithelial cells to the water-soluble and organic-soluble fractions of OA from wood pyrolysis. They showed that the more oxidized water-soluble OA fraction induced more oxidative stress and apoptosis but less DNA damage than the less oxidized organic-soluble fraction. Furthermore, the chemical composition of biomass-burning PM varies with fuel type and combustion conditions[34]. Kim et al.[35] exposed mice to emissions from burning of peat, eucalyptus, and oak at either smoldering or flaming combustion conditions and reported inflammation levels that were dependent on fuel type, with higher levels associated with peat and eucalyptus compared to oak. That study also reported that even though flaming emissions contained less PM than smoldering emissions, the flaming PM induced higher levels of toxicity per unit mass of PM.

After it is emitted to the atmosphere, biomass-burning PM evolves significantly upon reacting with oxidants such as hydroxyl radicals (OH)[36-38] and secondary organic aerosol (SOA) formation from the oxidation and subsequent condensation of the co-emitted organic vapors[39, 40]. SOA from both biogenic (α-pinene) and anthropogenic (m-xylene, naphthalene) precursors was shown to reduce metabolic activity of human lung epithelial cells[41], generate reactive oxygen and nitrogen species (ROS / RNS) in murine alveolar macrophages[42, 43], as well as induce oxidative stress and inflammation in human lung epithelial cells and macrophages[44]. However, the effect of atmospheric photochemical aging and SOA formation on biomass-burning PM toxicity is understudied and has only been investigated in the context of the oxidative potential (OP) using the dithiothreitol (DTT) chemical assay[45, 46]. Wong et al. used field and laboratory data to compare the effect of atmospheric transport time (in the field) and different aging mechanisms (in the laboratory) on the OP of biomass-burning PM[45]. They reported a 50% increase in the OP after a few hours of atmospheric transport, with relatively stable OP after that. In their laboratory experiments, however, they found that the aging of biomass-burning PM by photolysis increased the OP initially, only to be followed by a decline. Aqueous OH oxidation, in contrast, led to a rapid significant decline in OP. Jiang and

Jang[46] measured the DTT activity of wood smoke PM over a period of several hours of photooxidation. They found that the photochemical aging of the PM led to a significant decrease in OP, which they attributed to the decomposition of oxidizers. Verma et al.[47] used an aerosol mass spectrometer to group ambient OA collected at different locations in the Southeastern United States according to identity / source. Using the DTT assay, they found that biomass-burning OA had the highest OP per mol. In previous work, Verma et al.[48] found that biomass-burning OA and SOA dominated the OP of ambient aerosol in the Southeastern United States, with strong seasonal dependence (biomass-burning OA in the winter, SOA in the summer). Although these studies highlight the importance of the toxicity of atmospherically aged biomass-burning PM, it remains unclear if / how atmospheric aging alters the toxicity mechanisms.

In this study, we exposed human lung epithelial cells *in vitro* to fresh and photochemically aged PM emitted from the combustion of three biomass fuels. We used two assays to assess the reduction in cell metabolic activity as well as cell death by apoptosis and necrosis. We also analyzed the PM chemically to investigate the relation between toxicity and chemical composition of fresh and aged PM.

2. Methods

2.1. Combustion Experiments

We burnt dead Pin oak (*Quercus palustris*) foliage, Pignut hickory (*Carya glabra*) twigs, and Slash pine (*Pinus elliottii*) needles, all fuels commonly consumed in wildland fires in the Southeastern United States[49, 50], inside a 7.5 m^3 environmental chamber. The environmental chamber was lined with 44 UV lamps (GE Blacklight F40BL) on the bottom. The light intensity in the chamber corresponds to NO_2 photolysis rate (J_{NO2}) of 0.41 min^{-1} (see Supplementary Information (SI) for details), which is within the range of environmental chamber designs reported in the literature[51, 52] and is slightly smaller than J_{NO2} = 0.49 min^{-1} for a sunny day, ground level, 40°N, July 1, noon, 25 °C[53]. Before each experiment, the chamber was conditioned to a relative humidity of approximately 50% to promote the production of OH radicals when the UV lights were turned on. We burnt 25 g of each fuel inside the environmental chamber, restricting the combustion to the smoldering (flameless) phase. By focusing the experiments on the smoldering phase of combustion, we ensured that there were minimal concentrations of black carbon and that the PM inside the chamber was largely soluble in methanol[54, 55], the importance of which is discussed below.

We measured the particle size distribution inside the chamber throughout the experiments using a scanning mobility particle sizer (SMPS, TSI 3882), covering particles in the range of 10-500 nm. The total PM mass concentration in the chamber was calculated by integrating the SMPS size distribution, with an assumed particle density of 1.2 g/cm^3 [56, 57]. After the UV lights were turned on, the PM concentration increased due to the production of SOA from the photooxidation and subsequent condensation of vapor species. We estimated the concentration of SOA produced by subtracting the fresh PM concentration (i.e., PM concentration before the lights were turned on) from the concentration after the lights were turned on. To do that, we accounted for particle losses to the chamber walls, as described in the SI. We collected fresh and aged PM on 47 mm Teflon filters (0.2 microns, Sterlitech Corporation, PTU024750) for chemical analysis and *in vitro* exposure. We collected four filters at a time with a flow rate of 5 SLPM through each. The aged PM was collected after 2 hours of photooxidation.

2.2. Sample Extraction for Chemical Analysis and *in vitro* Exposure

We extracted the filters collected under each condition in 10 ml of methanol inside a glass vial, sonicating the vial for 10 minutes. We then removed the Teflon filters and filtered the solution in a glass syringe with

121 a metal luer lock tip through a 13 mm Teflon filter (0.2 microns, Sterlitech Corporation, PTU021350) to
122 remove suspended particles, since those could create nonuniformities in the *in vitro* exposure tests[58, 59].
123 As mentioned earlier, restricting the combustion experiments to the smoldering phase reduces the
124 amount of methanol-insoluble species, such as black carbon, that would be filtered out in this process.
125 Thus, the species extracted in methanol were largely representative of the PM in the chamber. At the end
126 of this process, we had six vials representing parent solutions for each of the conditions under study (three
127 biomass fuels, fresh and aged PM from each).

128 Inorganic salts and metals constitute a small fraction of biomass-burning PM mass, usually less than 5%[27,
129 60] . Therefore, the PM concentration in the solutions was mostly dictated by organics. We determined the
130 organic carbon concentration in the solutions using an organic-carbon elemental-carbon (OCEC) analyzer
131 (Sunset Laboratory Inc, model 4L) running the NIOSH-870 protocol[61]. The OCEC analyzer measures the
132 total amount of carbon on a Quartz filter punch by heating the sample at different temperature stages
133 and then measuring the carbon species, as CO_2, using a non-dispersive infrared sensor. To measure the
134 concentration of carbon in the solutions, we pipetted 200 µL of each solution onto a pre-baked 1.5 cm^2
135 punch in 50 µL steps. After each step, we evaporated the methanol under a stream of clean, dry air. To
136 estimate the concentration of the parent solutions, we divided the total OC measured by the OCEC
137 analyzer by the volume pipetted onto the Quartz filter punch (200 µL).

138 The PM solutions were then used for chemical analysis and *in vitro* exposure as elaborated in the
139 subsequent sections. We also prepared a background sample consisting of a blank Teflon filter extracted
140 and filtered in the same procedure as the combustion samples.

141 **2.3 Chemical Analysis**

142 We used ultra-high resolution electrospray ionization mass spectrometry (ESI-MS) to chemically
143 characterize the OA in the samples. The mass spectra of the samples were obtained using a Bruker SolariX
144 XR 12T Fourier-transform ion cyclotron resonance (FTICR) in positive ionization mode. Peaks were picked
145 using the open-source software mMass (mmass.org) with a signal-to-noise ratio of 3. Background peaks
146 (i.e., those appearing for a blank Teflon filter extracted in methanol) were excluded from the sample peaks
147 with a tolerance of 1 ppm. We used Formularity[62, 63], an automated formula assignment software, to
148 identify probable molecular formulae with the following constraints[33]: ±3 ppm, $C_{6\text{-}50}H_{6\text{-}100}N_{0\text{-}2}O_{0\text{-}12}S_{0\text{-}1}$.

149 Metals are common components in biomass-burning PM emissions, and their toxicity in trace
150 concentrations has been repeatedly demonstrated[64-66]. We analyzed the PM samples for metal content
151 using induction-coupled plasma mass spectrometry (ICP-MS). One half of a Teflon filter corresponding to
152 the fresh PM samples from each combustion experiment was transferred into a Teflon digestion vessel
153 and treated with 5 ml of trace-metal grade nitric acid. The vessel was then subjected to microwave
154 digestion, following EPA protocol[67]. After cooling to room temperature, the vessels were opened, treated
155 with 20 ml of water, and shaken thoroughly. Finally, 1 ml from each vessel was diluted to 10 ml with 1%
156 nitric acid and analyzed using the ICP-MS (Perkin Elmer Elan 9000) according to EPA method 200.8
157 protocol[68].

158 **2.4 Cell Preparation and Exposure Doses**

159 Cell cultures were prepared by growing immortalized human bronchial epithelial cells (cell line BEAS-2B
160 (ATCC: CRL-9609) obtained from the American Tissue Culture Collection (ATCC, Manassas, VA, 20110)) in

a treated cell culture grade T75-flask with Bronchial Lung Epithelial Basal Cell medium complete with growth factors and nutrients (Lonza BEGM™), herein referred to as complete BEBM. The cell culture was kept at 37°C in a humidified environment with 5% CO_2 until a confluence of 70-80 % was reached, after which the cells were split enzymatically by a 5-minute incubation in 0.18% trypsin (and 0.5 mM EDTA) followed by centrifugation at 200 relative centrifugal force (RCF) for five minutes. The supernatant was discarded, and fresh medium was added to the cell pellet. The cells were counted by trypan blue assay using an automated Cell Counter (Nano EnTek).

We prepared 5 exposure doses of the fresh and aged PM. To do so, we added different volumes from the parent PM solutions into vials, allowed the methanol to evaporate completely, and re-dissolved the PM in deionized (DI) water with 1% dimethyl sulfoxide (DMSO). The resulting PM concentrations were 20, 200, 550, 900, and 2150 µg-PM/ml. We also prepared a solvent control solution of DI water with 1% DMSO. The solutions were diluted by a factor of 10 upon introduction to the cell cultures, resulting in exposure doses of 0 (solvent control), 2, 20, 55, 90, and 215 µg-PM/ml, and 0.1% DMSO concentration at exposure. The exposure doses cover a wide range (2 orders of magnitude), which overlaps with doses in previous studies on PM toxicity[33, 41, 69]. The dose-response behavior of cells upon exposure to PM typically exhibits sigmoidal profiles. Based on preliminary experiments, we expected the linear portion of the response to be in the 10 – 100 µg-PM/ml, with the response plateauing at doses > 100 µg-PM/ml. Therefore, these doses were chosen to to maximize the potential for capturing the dose-response behavior of the cells.

2.5 WST-8 Assay

We assessed the metabolic activity of the cells using a tetrazolium salt-based colorimetric WST-8 assay (2-(2-methoxy-4-nitrophenyl)-3-(4-nitrophenyl)-5-(2,4-disulfophenyl)-2H-tetrazolium, monosodium salt)) using the Cell Counting Kit-8 (CCK-8, Sigma Aldrich). The cleavage of the salt by metabolically active cells leads to the formation of formazan, the concentration of which can be measured optically due to its light absorption at 450 nm. Thus, higher absorption at 450 nm corresponds to higher metabolic activity.

We added 10 µl of the PM in DI water + 1% DMSO samples to 90 µl of complete BEBM + cells (10^4 cells/well) in 96-well plates. We conducted exposure doses of 0 (control), 2, 20, 55, 90, and 215 µg-PM/ml. Cell density can influence the biologically effective dose[70], and there is evidence that per-cell basis is potentially a more appropriate dose metric[71]. For a cell density of 10^5 cells/ml (10^4 cells/well), the corresponding per-cell doses are 0 (solvent control), 20, 200, 550, 900, and 2150 pg-PM/cell. The exposures were performed in pentaplicates. After a 24-hour incubation period, we used a plate reader (Cytation 5, Biotek, Winooski, VT) to measure the background absorption of the treated cells at 450 and 650 nm prior to adding the WST-8 assay. When adding the WST-8 assay solution, the existing media was replaced with 10% WST-8 assay tetrazolium-salt solution in complete BEBM. The plates were left to incubate at 37°C, 5% CO_2 for 2 hours to allow for the reduction reaction to take place. We then used the Cytation-5 plate reader to measure the absorption again at 450 and 650 nm, corresponding to the formazan and formazan-free absorption, respectively. We measured the absorption before and after adding the WST-8 assay to account for possible light absorption by the OA, which could be confounded with the absorption by formazan. We calculated the metabolic activity in each well as:

$$\text{Metabolic Activity (\%)} = 100 \times \frac{(\text{sample}_{450} - \text{sample}_{\text{bkg},450}) - (\text{sample}_{650} - \text{sample}_{\text{bkg},650})}{(\text{control}_{450} - \text{control}_{\text{bkg},450}) - (\text{control}_{650} - \text{control}_{\text{bkg},650})} \quad (1)$$

Here, the $sample_{\lambda}$ corresponds to the absorption at wavelength λ = 450 nm or 650 nm after the addition of WST-8, whereas $sample_{bkg,\lambda}$ corresponds to the absorption measured prior to the addition of WST-8. The same applies to $control_{\lambda}$ and $control_{bkg,\lambda}$.

2.6 Annexin V Assay

We assessed cell death induced by apoptosis and necrosis using the Muse® Annexin V and Dead Cell Assay Kit (Luminex). The kit uses 7-Aminoactinomycin D (7-AAD) to distinguish late apoptotic cells from necrotic ones. We added 100 µl of the PM in DI water + 1% DMSO samples to 900 µl of complete BEBM + cells (2.5 x 10^5 cells/well) in 12-well plates. We conducted exposure doses of 0 (solvent control), 20, 55, and 215 µg-PM/ml, which correspond 0 (solvent control), 80, 220, and 860 pg-PM/cell. After 24-hour incubation, the cells were harvested and stained according to the manufacturer's instructions. Due to the limited amount of PM samples, we only performed single exposures with Annexin V, which did not allow for statistical comparison across fuels. As described in Section 3.2, we averaged the Annexin V results for the three fuels, which allowed for comparison between the fresh and aged PM.

2.7 Statistics

We conducted analysis of variance (ANOVA) followed by the Bonferroni post-hoc test to determine significant differences across different groups. Significant differences are reported as $p < 0.05$. We further fit the metabolic activity data (WST-8 assay) to a 5th degree exponential function using EPA's BMDS 3.2 tool (https://www.epa.gov/bmds) and determined the half-maximal inhibitory concentration IC_{50}, i.e., the dose that causes a 50% reduction in metabolic activity.

3. Results and Discussion

3.1. Chemical Composition of the Fresh and Photochemically Aged Organic Aerosol

The time series of the PM mass concentration in the environmental chamber produced from the combustion of hickory twigs is shown in Figure 1. Those from the combustion of pine needles and oak foliage are shown in Figure S1. At $t < 0$, the PM mass concentration decays due to particle wall loss in the chamber. At $t = 0$, when the UV lights were turned on, a reversal in the decay of PM mass concentration is observed due to the production of SOA. The OA enhancement, or the fold increase in PM concentration due to the mass contributed by SOA[72], was approximately 1.46 for hickory, 1.42 for oak, and 1.21 for pine. We note that the chemical transformation of the OA is not restricted to the production of SOA from the oxidation of volatile species. Heterogeneous oxidation reactions can also alter the chemical composition of OA in the particle phase[38], though to a lesser extent than SOA formation[60]. Furthermore, the temperatures in smoldering combustion are not high enough to produce significant amounts of NO_x[73]. Therefore, we expect O_3 production to be negligible[74] and OH oxidation to be the dominant driver of the OA chemical transformation.

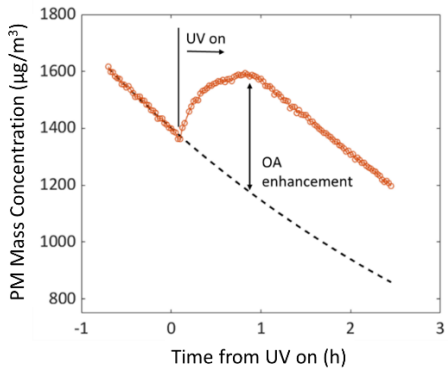

Figure 1. The evolution of PM mass concentration in the chamber for the hickory twigs combustion experiment. At t = 0, the UV lights were turned on, which marks the onset of photochemical aging of the emissions. The black dashed line is the exponential decay fit to the fresh PM mass concentration, used to estimate the OA enhancement due to SOA formation (see SI for details).

The mass spectra of the fresh and aged OA, obtained using ESI-MS, are shown in Figure S2. The compounds identified include species that are common markers for, or have been identified in, biomass-burning OA such as levoglucosan ($C_6H_{10}O_5$)[26, 75-77], fructose ($C_6H_{12}O_6$)[78, 79], diethyl phthalate ($C_{12}H_{14}O_4$)[80, 81], and dibutyl phthalate ($C_{16}H_{22}O_4$)[80, 81]. It is important to note that biomass-burning OA species are detected at different efficiencies by ESI-MS. For example, compounds with low polarity such as polycyclic aromatic hydrocarbons (PAHs) and their oxygenated derivatives (oxy-PAHs) are detected at relatively low efficiencies[82]. Differences in the chemical composition across fuels and between the fresh and aged OA detected by ESI-MS are illustrated using Van-Krevelen diagrams in Figure 2. As expected, OA from all fuels became more oxidized upon aging[37, 38], where the species unique to the aged OA (either SOA or heterogeneously oxidized OA) generally have larger O:C than the species unique to the fresh OA. As shown in Table 1, this is reflected in an increase in the average O:C as well as the ratio of organic matter (OM) to organic carbon (OC), OM:OC upon aging, in a fashion consistent with previous reports[39 83].

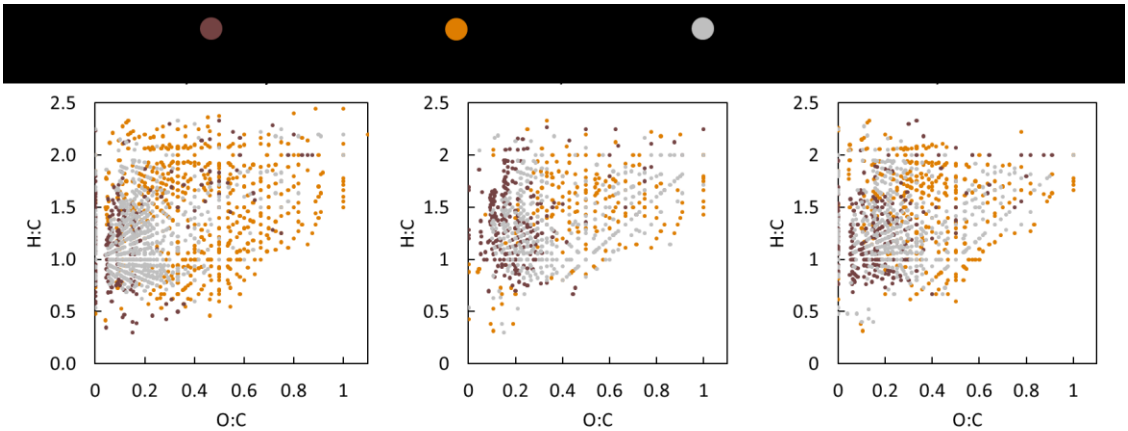

Figure 2. Van-Krevelen plots showing O:C versus H:C of the compounds detected by ESI-MS in the fresh and photochemically aged OA from the combustion of different fuels.

Table 1. Average O:C, OM:OC, and AI_{mod} of the compounds detected by ESI-MS in the fresh and photochemically aged OA from the combustion of different fuels.

	Average O:C	Average OM:OC	Average AI_{mod}
Fresh hickory	0.25	1.50	0.31
Aged hickory	0.33	1.61	0.19
Fresh pine	0.32	1.56	0.25
Aged pine	0.41	1.70	0.15
Fresh oak	0.24	1.50	0.30
Aged oak	0.30	1.59	0.18

We also calculated the modified aromaticity index[84, 85] (AI_{mod}) of the organic species detected by ESI-MS as $\mathrm{AI_{mod}} = \frac{1+c-o-0.5n-0.5h}{c-0.5o-n}$, where c, o, h, and n correspond to the number of C, O, H, and N atoms. AI_{mod} > 0.5 and AI_{mod} > 0.67 correspond to aromatic structures and condensed aromatic structures, respectively. Table 1 shows the average AI_{mod} values of fresh and photochemically aged OA from all fuels, which are within the range of AI_{mod} (0.29 ± 0.27) reported for ambient biomass-burning OA[86]. As expected, AI_{mod} decreased with aging indicating that the fresh OA had a higher aromaticity[87]. This is further illustrated in Figure 3, which shows that the relative abundance of aromatic and condensed aromatic species decreased with photochemical aging for all fuels.

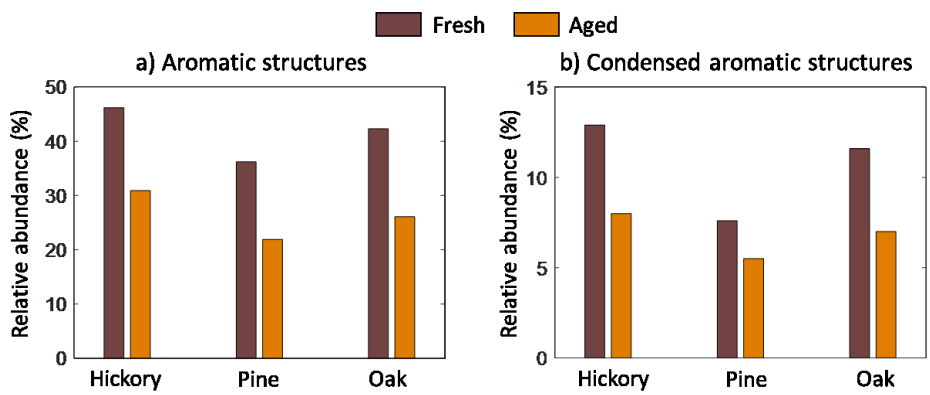

Figure 3. Relative abundance of (a) aromatic structures, corresponding to modified aromaticity index (AI_{mod}) > 0.5 and (b) condensed aromatic structures, corresponding to AI_{mod} > 0.67 in the fresh and photochemically aged OA species detected by ESI-MS for the different fuels.

3.2. Cell Death and Reduction in Metabolic Activity

Figure 4 shows the cell metabolic activity obtained using the WST-8 assay after 24-hour exposure to each of the fresh and photochemically aged PM from the three fuels. All samples exhibited typical dose-response profiles, with a significant decrease in metabolic activity relative to solvent control at all exposure doses equal to or higher than 20 µg-PM/ml (200 pg-PM/cell). The results in Figure 4 reflect the dependence of metabolic activity on both fuel type and photochemical aging. These trends can be conveniently summarized using the half-maximal inhibitory concentration, IC_{50}, which is the dose that causes a 50% reduction in metabolic activity. There are significant differences in IC_{50} across the fresh PM samples, with the fresh PM from hickory combustion having the smallest IC_{50}, followed by pine and oak. For all fuels, the IC_{50} of the fresh PM was significantly smaller than the IC_{50} of the aged PM, indicating that photochemical aging rendered the PM less potent at reducing the metabolic activity of the cells.

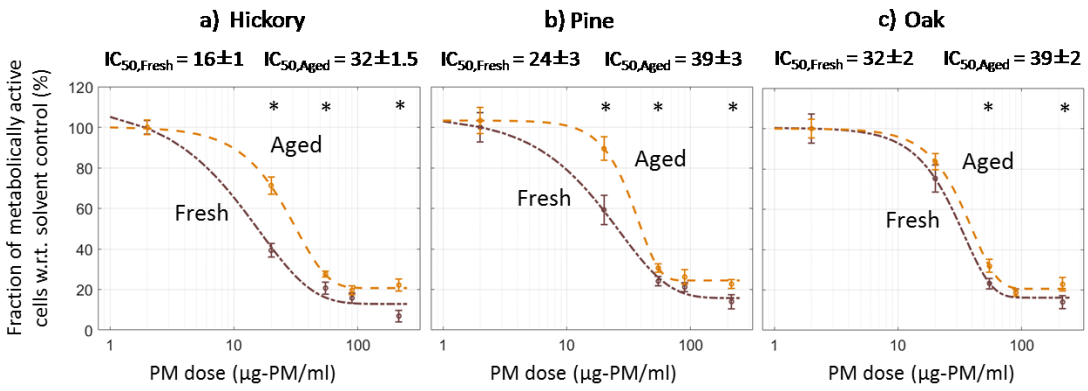

Figure 4. Results from the WST-8 assay showing metabolic activity relative to solvent control of cells exposed to fresh and photochemically aged PM from the combustion of different fuels. Error bars represent standard deviations from five measurements. Significant differences with solvent control were obtained for all fresh and aged PM exposures at doses ≥ 20 µg-PM/ml. Significant differences between fresh and aged PM are denoted by asterisks. The dashed lines represent 5th degree exponential fits calculated using BMDS 3.2. Above the panel for each fuel is its IC_{50}, the dose required for a 50% reduction in cell metabolic activity, and the 95% confidence interval.

However, with further investigation of cell death pathways, the results become more nuanced. Figure 5 shows the flow cytometry results from the Annexin V assay of cells exposed to 55 µg-PM/ml (220 pg-PM/cell) for 24 hours of fresh and aged biomass-burning PM from the different fuels. The results for cells exposed to 20 µg-PM/ml (80 pg-PM/cell) and 215 µg-PM/ml (860 pg-PM/cell) are shown in Figures S3 and S4, respectively. The flow cytometry analysis identifies cells that are live, early apoptotic, late apoptotic, and dead, with each category falling in a unique quadrant in the panels shown in Figure 5. In contrast to the WST-8 assay, the Annexin V assay shows increasing toxicity with the photochemical aging of the PM, with the aged PM inducing higher levels of late apoptosis than the fresh PM across all fuels.

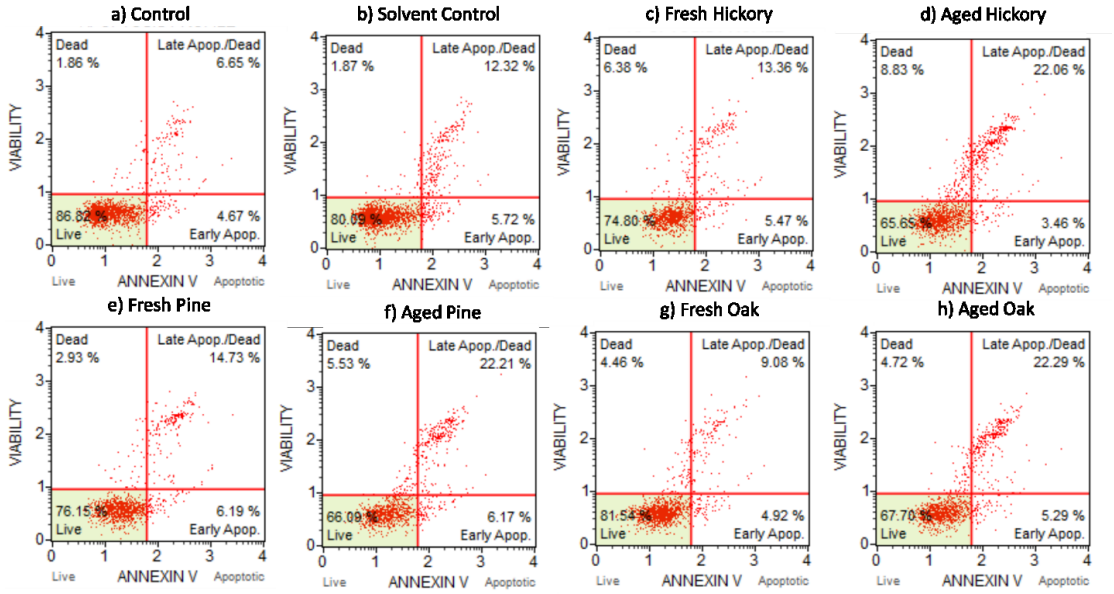

Figure 5. Flow cytometry analysis of cells exposed to 55 µg-PM/ml of fresh and photochemically aged PM from the combustion of different fuels. Also shown are data for control (untreated cells) and solvent control (cells exposed to DI water + 0.1% DMSO). The quadrants indicate the fractions of live, early apoptotic, late apoptotic, and dead/necrotic cells.

Constrained by the amount of PM samples, we were able to perform only one measurement for each exposure with the Annexin V assay, which did not allow for statistical comparison across fuels. However, the measurements from the three fuels can be combined to perform comparison between the fresh and aged PM. As shown in Figure 6, averaged over the three fuels, the aged PM induced higher levels of apoptosis and necrosis than the fresh PM, with the exception of necrosis at 20 µg-PM/ml (80 pg-PM/cell), with significant differences in apoptosis at 20 µg-PM/ml (80 pg-PM/cell) and 55 µg-PM/ml (220 pg-PM/cell).

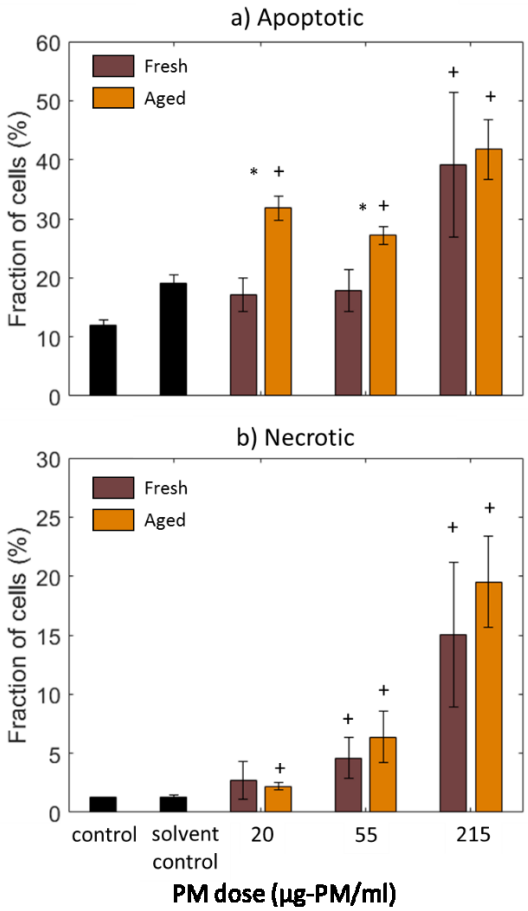

Figure 6. The fraction of (a) total apoptotic and (b) necrotic cells after exposure to fresh and photochemically aged PM averaged across all fuels. Also shown are data for control (untreated cells) and solvent control (cells exposed to DI water + 0.1% DMSO). Error bars represent standard deviations from 3 measurements (one for each fuel). Significant differences relative to solvent control are denoted by plus signs. Significant differences between the fresh and aged samples are denoted by asterisks.

Comparison of the response of the cells assessed using the WST-8 and Annexin V assays to fresh and photochemically aged PM, averaged across all fuels, is shown in Figure 7. While the fresh PM was more

potent at reducing the metabolic activity of the cells, the aged PM induced more cell death. The seeming inconsistency between the WST-8 and Annexin V assays is potentially a manifestation of differences in toxicity mechanisms that are captured by the different end points measured by the two assays. The Annexin V assay measures apoptosis and necrosis by detecting exofacial phosphatidylserine (annexin V) and permeable cell membranes (7-AAD), each distinct markers for apoptotic and necrotic cells, respectively[88, 89]. However, other programmed cell death pathways[90] with different markers can go undetected with the Annexin V. Those pathways could lead to a reduction in metabolic activity, which can also be cell-death independent[91].

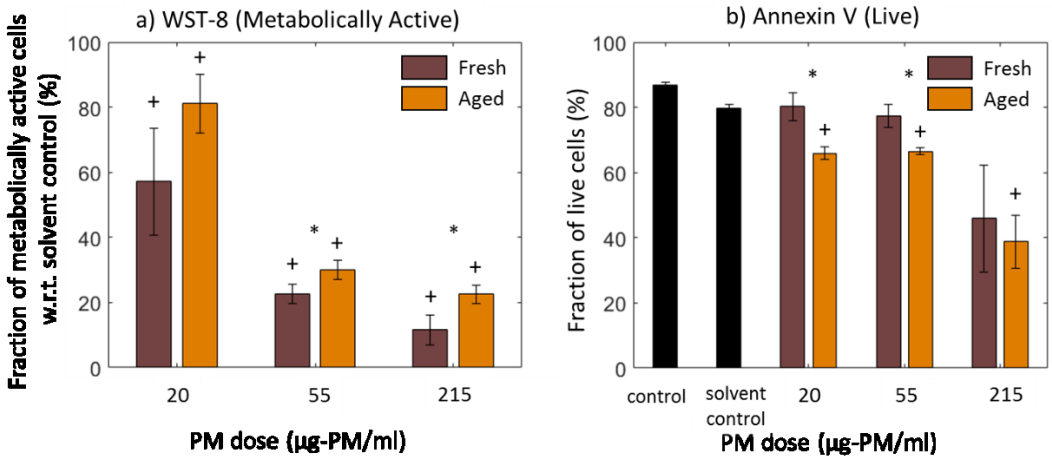

Figure 7. The fraction of (a) metabolically active cells relative to solvent control (WST-8) and (b) live cells (Annexin V) after exposure to fresh and photochemically aged PM averaged across all fuels. Also shown are data for control (untreated cells) and solvent control (cells exposed to DI water + 0.1% DMSO) for Annexin V. Error bars represent standard deviations from 15 measurements (5 for each fuel) in panel (a) and 3 measurements (one for each fuel) in panel (b). Significant differences between the fresh and aged samples are denoted by asterisks. In panel (b), significant differences relative to solvent control are denoted by plus signs.

Different OA species can induce different toxicity mechanisms[92]. Pardo et al.[33] separated tar distilled from wood pyrolysis (equivalent to the fresh OA in this study) into water-soluble and organic-soluble fractions. They found that the water-soluble fraction, which is more oxygenated (has higher O:C) but has a lower aromatic content than the organic-soluble fraction, caused more oxidative stress and apoptosis but less DNA damage in lung epithelial cells. The difference in toxicity mechanisms between the water-soluble and organic-soluble fractions in Pardo et al. is possibly driven by the relative abundance of oxidized organic species and aromatic structures in the two fractions. It is plausible that the relative abundance of oxidized organic species also plays a role in the differences in cellular responses between fresh and aged PM in this study. Photochemical aging increases the abundance of highly oxidized species (Figure 2), which renders the PM more potent at producing ROS and inducing apoptosis mediated by oxidative stress. On the other hand, photochemical aging decreases the abundance of aromatic and condensed aromatic structures (Figure 3), which renders the PM less potent at inducing DNA damage. Excessive activation of Poly(ADP-ribose) polymerase-1 (PARP-1) proteins in response to DNA damage[93] has been shown to reduce metabolic activity without necessarily causing cell death[91]. This could partly explain the lower metabolic activity for the fresh PM despite the higher rate of cell death for the aged PM (Figure 7).

347 In general, these results indicate that even for the relatively short chamber oxidation time in our
348 experiments (2 hours), photochemical aging significantly alters the toxicity mechanisms induced by the
349 PM. Longer OH exposure continues to chemically transform the PM over time scales of days[60], which is
350 expected to further affect PM toxicity. Furthermore, biomass-burning plumes undergo other oxidation
351 pathways, including ozonolysis[34] and nighttime oxidation with nitrate radicals[94], that can potentially have
352 different impacts on the biomass-burning PM toxicity.

353 **3.3. Possible Competing Roles of Heavy Metals and Organic Aerosol**

354 Biomass-burning PM and atmospheric PM in general usually contain trace amounts of heavy metals. Even
355 though heavy metals typically constitute < 0.1% of the PM mass, they are important contributors to PM
356 toxicity, as has been confirmed in *in vitro* exposure studies[95]. Heavy metals in ambient PM have been
357 associated with adverse health outcomes and have been shown to exhibit positive mortality risk
358 coefficients[96]. We detected several heavy metals with established toxicities in the PM samples (Table 2).
359 The differences in PM metal content across fuels should not be taken as a characteristic of each fuel, as
360 these metals could have originated from various natural and/or anthropogenic sources and then absorbed
361 by the biomass[97, 98]. We note the samples used in ICP-MS measurements to obtain the values in Table 2
362 were prepared using nitric acid extraction, while the PM samples for cell exposure were prepared using
363 methanol extraction. Therefore, even though methanol is effective at extracting metals[99, 100], it is likely
364 that there are differences in the metal content values in Table 2 and the metal content in the PM used for
365 cell exposure. Nevertheless, metal toxicity can partly explain the differences in metabolic activity across
366 fuels. Hickory PM had the highest overall metal content (3.25 mg/g-PM), followed by pine (0.49 mg/g-PM)
367 and oak (0.39 mg/g-PM), which is in line with their differential reduction in metabolic activity (Figure 4).
368 Furthermore, arsenic and thallium, both considered among the more toxic heavy metals[101, 102], were only
369 detected in hickory PM.

370 **Table 2.** Heavy metals content in the fresh PM from the combustion of different fuels obtained using ICP-
371 MS. The analysis also included iron (Fe), copper (Cu), and lead (Pb), but those were not detected in any of
372 the samples.

	Hickory	**Pine**	**Oak**
Metal	**Metal Content (mg/g-PM)**		
Arsenic (As)	0.56	ND	ND
Cadmium (Cd)	0.03	0.01	0.01
Chromium (Cr)	ND	0.48	0.38
Antimony (Sb)	0.27	ND	ND
Thallium (Tl)	2.39	ND	ND

373

374 Mitochondrial dysfunction induced by metals[102-104] can also partly explain the lower metabolic activity in
375 the fresh PM compared to aged PM. SOA formation upon photochemical aging increases the PM
376 concentration and effectively dilutes the metal content in the aged PM relative to the fresh PM. Thus, for
377 the same PM exposure dose, the cells were exposed to higher levels of metals in the fresh PM compared
378 to the aged PM. However, photochemical aging of the PM led to increased apoptotic cell death (Figure 6)
379 despite the reduction in metal content, which suggests a more dominant role of increased OA oxygenation
380 at inducing these endpoints. Similar to OA, heavy metals have been implicated in various toxicity
381 mechanisms that can contribute to the observed cell death and decreased metabolic activity in this study,

including oxidative stress[105, 106], inhibition of DNA repair[104], excessive PARP-1 activation[105], and mitochondrial dysfunction[105, 107]. It is plausible that metals are more efficient at inducing effects that are more linked to metabolic activity (mitochondrial dysfunction), while increased OA oxygenation upon photochemical aging renders the PM more efficient at inducing effects more linked to apoptosis (e.g., oxidative stress).

4. Conclusions

Human bronchial epithelial cells exhibited different responses when exposed to fresh and photochemically aged PM emitted from the combustion of hickory twigs, pine needles, and oak foliage. Hickory PM induced the strongest reduction in metabolic activity, followed by pine and oak. While the limited number of fuels investigated in this study does not allow for deriving generalized correlations between fuel type and levels of smoke toxicity, our results suggest that smoke toxicity depends on fuel type. The aged PM induced more apoptotic cell death, while the fresh PM was more potent at reducing metabolic activity. These results indicate that atmospheric processing alters the toxicity of biomass-burning PM in a complex fashion, with a possible important contribution by heavy metals. This calls for targeted efforts to investigate the effect of aging on the underlying toxicity mechanisms implicated in the observed endpoints in this study. These could include focusing on specific biological markers related to mitochondrial function[108-111], as well as elucidating causal pathways between intracellular responses (e.g. oxidative stress, PARP-1 overactivation) and cell death[91].

Funding Sources

This work was supported by the National Science Foundation, Division of Atmospheric and Geospace Sciences [AGS-1748080].

Acknowledgments

The ESI-MS chemical analysis of the organic aerosol was performed at the University of Georgia Proteomics and Mass Spectrometry Core Facility and the ICP-MS metals analysis was performed at the University of Georgia Laboratory for Environmental Analysis.

References

1. Hiers, J. K.; O'Brien, J. J.; Varner, J. M.; Butler, B. W.; Dickinson, M.; Furman, J.; Gallagher, M.; Godwin, D.; Goodrick, S. L.; Hood, S. M., Prescribed fire science: the case for a refined research agenda. *Fire Ecology* **2020,** *16* (1), 1-15.
2. O'Brien, J.; Hiers, J.; Varner, J.; Hoffman, C.; Dickinson, M.; Michaletz, S.; Loudermilk, E.; Butler, B., Advances in mechanistic approaches to quantifying biophysical fire effects. *Current Forestry Reports* **2018,** *4* (4), 161-177.
3. Sokolik, I.; Soja, A.; DeMott, P.; Winker, D., Progress and challenges in quantifying wildfire smoke emissions, their properties, transport, and atmospheric impacts. *Journal of Geophysical Research: Atmospheres* **2019,** *124* (23), 13005-13025.
4. Dong, X.; Fu, J. S.; Huang, K.; Zhu, Q.; Tipton, M., Regional climate effects of biomass burning and dust in East Asia: evidence from modeling and observation. *Geophysical Research Letters* **2019,** *46* (20), 11490-11499.
5. Thornhill, G. D.; Ryder, C. L.; Highwood, E. J.; Shaffrey, L. C.; Johnson, B. T., The effect of South American biomass burning aerosol emissions on the regional climate. *Atmospheric Chemistry and Physics* **2018,** *18* (8), 5321-5342.

6. Saleh, R.; Marks, M.; Heo, J.; Adams, P. J.; Donahue, N. M.; Robinson, A. L., Contribution of brown carbon and lensing to the direct radiative effect of carbonaceous aerosols from biomass and biofuel burning emissions. *Journal of Geophysical Research: Atmospheres* **2015,** *120* (19).

7. Fann, N.; Alman, B.; Broome, R. A.; Morgan, G. G.; Johnston, F. H.; Pouliot, G.; Rappold, A. G., The health impacts and economic value of wildland fire episodes in the US: 2008–2012. *Science of the total environment* **2018,** *610*, 802-809.

8. Cascio, W. E., Wildland fire smoke and human health. *Science of the total environment* **2018,** *624*, 586-595.

9. Dennekamp, M.; Straney, L. D.; Erbas, B.; Abramson, M. J.; Keywood, M.; Smith, K.; Sim, M. R.; Glass, D. C.; Del Monaco, A.; Haikerwal, A., Forest fire smoke exposures and out-of-hospital cardiac arrests in Melbourne, Australia: a case-crossover study. *Environmental health perspectives* **2015,** *123* (10), 959-964.

10. Jaffe, D. A.; O'Neill, S. M.; Larkin, N. K.; Holder, A. L.; Peterson, D. L.; Halofsky, J. E.; Rappold, A. G., Wildfire and prescribed burning impacts on air quality in the United States. *Journal of the Air & Waste Management Association* **2020,** *70* (6), 583-615.

11. Larsen, A. E.; Reich, B. J.; Ruminski, M.; Rappold, A. G., Impacts of fire smoke plumes on regional air quality, 2006–2013. *Journal of exposure science & environmental epidemiology* **2018,** *28* (4), 319-327.

12. Knowlton, K., Where there's fire, there's smoke: wildfire smoke affects communities distant from deadly flames. *NRDC Issue Brief* **2013**.

13. Rappold, A. G.; Reyes, J.; Pouliot, G.; Cascio, W. E.; Diaz-Sanchez, D., Community vulnerability to health impacts of wildland fire smoke exposure. *Environmental Science & Technology* **2017,** *51* (12), 6674-6682.

14. Flannigan, M. D.; Krawchuk, M. A.; de Groot, W. J.; Wotton, B. M.; Gowman, L. M., Implications of changing climate for global wildland fire. *International journal of wildland fire* **2009,** *18* (5), 483-507.

15. Goss, M.; Swain, D. L.; Abatzoglou, J. T.; Sarhadi, A.; Kolden, C. A.; Williams, A. P.; Diffenbaugh, N. S., Climate change is increasing the likelihood of extreme autumn wildfire conditions across California. *Environmental Research Letters* **2020,** *15* (9), 094016.

16. Aguilera, R.; Corringham, T.; Gershunov, A.; Benmarhnia, T., Wildfire smoke impacts respiratory health more than fine particles from other sources: observational evidence from Southern California. *Nature communications* **2021,** *12* (1), 1-8.

17. Delfino, R. J.; Brummel, S.; Wu, J.; Stern, H.; Ostro, B.; Lipsett, M.; Winer, A.; Street, D. H.; Zhang, L.; Tjoa, T., The relationship of respiratory and cardiovascular hospital admissions to the southern California wildfires of 2003. *Occupational and environmental medicine* **2009,** *66* (3), 189-197.

18. Johnston, F. H.; Webby, R. J.; Pilotto, L. S.; Bailie, R. S.; Parry, D. L.; Halpin, S. J., Vegetation fires, particulate air pollution and asthma: a panel study in the Australian monsoon tropics. *International journal of environmental health research* **2006,** *16* (6), 391-404.

19. Adetona, O.; Reinhardt, T. E.; Domitrovich, J.; Broyles, G.; Adetona, A. M.; Kleinman, M. T.; Ottmar, R. D.; Naeher, L. P., Review of the health effects of wildland fire smoke on wildland firefighters and the public. *Inhalation toxicology* **2016,** *28* (3), 95-139.

20. Black, C.; Tesfaigzi, Y.; Bassein, J. A.; Miller, L. A., Wildfire smoke exposure and human health: Significant gaps in research for a growing public health issue. *Environmental toxicology and pharmacology* **2017,** *55*, 186-195.

21. Wu, C.-M.; Adetona, A.; Song, C.; Naeher, L.; Adetona, O., Measuring acute pulmonary responses to occupational wildland fire smoke exposure using exhaled breath condensate. *Archives of environmental & occupational health* **2020,** *75* (2), 65-69.

22. Wu, C.-M.; Warren, S. H.; DeMarini, D. M.; Song, C. C.; Adetona, O., Urinary mutagenicity and oxidative status of wildland firefighters working at prescribed burns in a Midwestern US forest. *Occupational and environmental medicine* **2021,** *78* (5), 315-322.

23. Scieszka, D.; Hunter, R.; Begay, J.; Bistui, M.; Lin, Y.; Galewsky, J.; Morishita, M.; Klaver, Z.; Wagner, J.; Harkema, J., Neuroinflammatory and neurometabolic consequences from inhaled 2020 California wildfire smoke-derived particulate matter at a remote location. **2021**.

24. Park, M.; Joo, H. S.; Lee, K.; Jang, M.; Kim, S. D.; Kim, I.; Borlaza, L. J. S.; Lim, H.; Shin, H.; Chung, K. H., Differential toxicities of fine particulate matters from various sources. *Scientific reports* **2018,** *8* (1), 1-11.

25. Pardo, M.; Li, C.; He, Q.; Levin-Zaidman, S.; Tsoory, M.; Yu, Q.; Wang, X.; Rudich, Y., Mechanisms of lung toxicity induced by biomass burning aerosols. *Particle and fibre toxicology* **2020,** *17* (1), 1-15.

26. Tuet, W. Y.; Liu, F.; de Oliveira Alves, N.; Fok, S.; Artaxo, P.; Vasconcellos, P.; Champion, J. A.; Ng, N. L., Chemical oxidative potential and cellular oxidative stress from open biomass burning aerosol. *Environmental Science & Technology Letters* **2019,** *6* (3), 126-132.

27. Akagi, S.; Yokelson, R. J.; Wiedinmyer, C.; Alvarado, M.; Reid, J.; Karl, T.; Crounse, J.; Wennberg, P., Emission factors for open and domestic biomass burning for use in atmospheric models. *Atmospheric Chemistry and Physics* **2011,** *11* (9), 4039-4072.

28. McClure, C. D.; Lim, C. Y.; Hagan, D. H.; Kroll, J. H.; Cappa, C. D., Biomass-burning-derived particles from a wide variety of fuels–Part 1: Properties of primary particles. *Atmospheric Chemistry & Physics* **2020,** *20* (3).

29. McMeeking, G. R.; Kreidenweis, S. M.; Baker, S.; Carrico, C. M.; Chow, J. C.; Collett Jr, J. L.; Hao, W. M.; Holden, A. S.; Kirchstetter, T. W.; Malm, W. C., Emissions of trace gases and aerosols during the open combustion of biomass in the laboratory. *Journal of Geophysical Research: Atmospheres* **2009,** *114* (D19).

30. Nelson, J.; Chalbot, M.-C. G.; Tsiodra, I.; Mihalopoulos, N.; Kavouras, I. G., Physicochemical characterization of personal exposures to smoke aerosol and PAHs of wildland firefighters in prescribed fires. *Exposure and Health* **2021,** *13* (1), 105-118.

31. Bluvshtein, N.; Lin, P.; Flores, J. M.; Segev, L.; Mazar, Y.; Tas, E.; Snider, G.; Weagle, C.; Brown, S. S.; Laskin, A., Broadband optical properties of biomass-burning aerosol and identification of brown carbon chromophores. *Journal of Geophysical Research: Atmospheres* **2017,** *122* (10), 5441-5456.

32. Jayarathne, T.; Stockwell, C. E.; Gilbert, A. A.; Daugherty, K.; Cochrane, M. A.; Ryan, K. C.; Putra, E. I.; Saharjo, B. H.; Nurhayati, A. D.; Albar, I., Chemical characterization of fine particulate matter emitted by peat fires in Central Kalimantan, Indonesia, during the 2015 El Niño. *Atmospheric Chemistry and Physics* **2018,** *18* (4), 2585-2600.

33. Pardo, M.; Li, C.; Fang, Z.; Levin-Zaidman, S.; Dezorella, N.; Czech, H.; Martens, P.; Käfer, U.; Gröger, T.; Rüger, C. P., Toxicity of Water-and Organic-Soluble Wood Tar Fractions from Biomass Burning in Lung Epithelial Cells. *Chemical research in toxicology* **2021**.

34. Tkacik, D. S.; Robinson, E. S.; Ahern, A.; Saleh, R.; Stockwell, C.; Veres, P.; Simpson, I. J.; Meinardi, S.; Blake, D. R.; Yokelson, R. J., A dual-chamber method for quantifying the effects of atmospheric perturbations on secondary organic aerosol formation from biomass burning emissions. *Journal of Geophysical Research: Atmospheres* **2017,** *122* (11), 6043-6058.

35. Kim, Y. H.; King, C.; Krantz, T.; Hargrove, M. M.; George, I. J.; McGee, J.; Copeland, L.; Hays, M. D.; Landis, M. S.; Higuchi, M., The role of fuel type and combustion phase on the toxicity of biomass smoke following inhalation exposure in mice. *Archives of toxicology* **2019**, 1-13.

36. Garofalo, L. A.; Pothier, M. A.; Levin, E. J.; Campos, T.; Kreidenweis, S. M.; Farmer, D. K., Emission and evolution of submicron organic aerosol in smoke from wildfires in the western United States. *ACS Earth and Space Chemistry* **2019,** *3* (7), 1237-1247.

37. Cappa, C. D.; Lim, C. Y.; Hagan, D. H.; Coggon, M.; Koss, A.; Sekimoto, K.; Gouw, J. d.; Onasch, T. B.; Warneke, C.; Kroll, J. H., Biomass-burning-derived particles from a wide variety of fuels–part 2: effects of photochemical aging on particle optical and chemical properties. *Atmospheric Chemistry and Physics* **2020,** *20* (14), 8511-8532.

38. Hodshire, A. L.; Akherati, A.; Alvarado, M. J.; Brown-Steiner, B.; Jathar, S. H.; Jimenez, J. L.; Kreidenweis, S. M.; Lonsdale, C. R.; Onasch, T. B.; Ortega, A. M., Aging effects on biomass burning aerosol mass and composition: A critical review of field and laboratory studies. *Environmental science & technology* **2019,** *53* (17), 10007-10022.

39. Ahern, A.; Robinson, E.; Tkacik, D.; Saleh, R.; Hatch, L.; Barsanti, K.; Stockwell, C.; Yokelson, R.; Presto, A.; Robinson, A., Production of secondary organic aerosol during aging of biomass burning smoke from fresh fuels and its relationship to VOC precursors. *Journal of Geophysical Research: Atmospheres* **2019,** *124* (6), 3583-3606.

40. Akherati, A.; He, Y.; Coggon, M. M.; Koss, A. R.; Hodshire, A. L.; Sekimoto, K.; Warneke, C.; de Gouw, J.; Yee, L.; Seinfeld, J. H., Oxygenated aromatic compounds are important precursors of secondary organic aerosol in biomass-burning emissions. *Environmental Science & Technology* **2020,** *54* (14), 8568-8579.

41. Chowdhury, P. H.; He, Q.; Lasitza Male, T.; Brune, W. H.; Rudich, Y.; Pardo, M., Exposure of lung epithelial cells to photochemically aged secondary organic aerosol shows increased toxic effects. *Environmental Science & Technology Letters* **2018,** *5* (7), 424-430.

42. Liu, F.; Saavedra, M. G.; Champion, J. A.; Griendling, K. K.; Ng, N. L., Prominent contribution of hydrogen peroxide to intracellular reactive oxygen species generated upon exposure to naphthalene secondary organic aerosols. *Environmental Science & Technology Letters* **2020,** *7* (3), 171-177.

43. Tuet, W. Y.; Chen, Y.; Fok, S.; Gao, D.; Weber, R. J.; Champion, J. A.; Ng, N. L., Chemical and cellular oxidant production induced by naphthalene secondary organic aerosol (SOA): effect of redox-active metals and photochemical aging. *Scientific reports* **2017,** *7* (1), 1-10.

44. Ito, T.; Bekki, K.; Fujitani, Y.; Hirano, S., The toxicological analysis of secondary organic aerosol in human lung epithelial cells and macrophages. *Environmental Science and Pollution Research* **2019,** *26* (22), 22747-22755.

45. Wong, J. P.; Tsagkaraki, M.; Tsiodra, I.; Mihalopoulos, N.; Violaki, K.; Kanakidou, M.; Sciare, J.; Nenes, A.; Weber, R. J., Effects of atmospheric processing on the oxidative potential of biomass burning organic aerosols. *Environmental science & technology* **2019,** *53* (12), 6747-6756.

46. Jiang, H.; Jang, M., Dynamic oxidative potential of atmospheric organic aerosol under ambient sunlight. *Environmental science & technology* **2018,** *52* (13), 7496-7504.

47. Verma, V.; Fang, T.; Xu, L.; Peltier, R. E.; Russell, A. G.; Ng, N. L.; Weber, R. J., Organic aerosols associated with the generation of reactive oxygen species (ROS) by water-soluble PM2. 5. *Environmental science & technology* **2015,** *49* (7), 4646-4656.

48. Verma, V.; Fang, T.; Guo, H.; King, L.; Bates, J.; Peltier, R.; Edgerton, E.; Russell, A.; Weber, R., Reactive oxygen species associated with water-soluble PM 2.5 in the southeastern United States: spatiotemporal trends and source apportionment. *Atmospheric Chemistry and Physics* **2014,** *14* (23), 12915-12930.

49. Zheng, M.; Cass, G. R.; Schauer, J. J.; Edgerton, E. S., Source apportionment of PM2. 5 in the southeastern United States using solvent-extractable organic compounds as tracers. *Environmental science & technology* **2002,** *36* (11), 2361-2371.

50. Fine, P. M.; Cass, G. R.; Simoneit, B. R., Chemical characterization of fine particle emissions from the fireplace combustion of woods grown in the southern United States. *Environmental Science & Technology* **2002,** *36* (7), 1442-1451.

51. Wang, X.; Liu, T.; Bernard, F.; Ding, X.; Wen, S.; Zhang, Y.; Zhang, Z.; He, Q.; Lü, S.; Chen, J., Design and characterization of a smog chamber for studying gas-phase chemical mechanisms and aerosol formation. *Atmospheric Measurement Techniques* **2014,** *7* (1), 301-313.

52. Li, K.; White, S.; Zhao, B.; Geng, C.; Halliburton, B.; Wang, Z.; Zhao, Y.; Yu, H.; Yang, W.; Bai, Z., Evaluation of a New Chemical Mechanism for 2-Amino-2-methyl-1-propanol in a Reactive Environment from CSIRO Smog Chamber Experiments. *Environmental Science & Technology* **2020,** *54* (16), 9844-9853.

53. Seinfeld, J.; Pandis, S., Atmospheric Chemistry and Physics. 1997. *New York* **2008**.
54. Li, X.; Chen, Y.; Bond, T. C., Light absorption of organic aerosol from pyrolysis of corn stalk. *Atmospheric Environment* **2016,** *144*, 249-256.
55. Chen, Y.; Bond, T., Light absorption by organic carbon from wood combustion. *Atmospheric Chemistry and Physics* **2010,** *10* (4), 1773-1787.
56. Sumlin, B. J.; Oxford, C. R.; Seo, B.; Pattison, R. R.; Williams, B. J.; Chakrabarty, R. K., Density and homogeneous internal composition of primary brown carbon aerosol. *Environmental science & technology* **2018,** *52* (7), 3982-3989.
57. Cross, E. S.; Slowik, J. G.; Davidovits, P.; Allan, J. D.; Worsnop, D. R.; Jayne, J. T.; Lewis, D. K.; Canagaratna, M.; Onasch, T. B., Laboratory and ambient particle density determinations using light scattering in conjunction with aerosol mass spectrometry. *Aerosol Science and Technology* **2007,** *41* (4), 343-359.
58. Verma, V.; Rico-Martinez, R.; Kotra, N.; King, L.; Liu, J.; Snell, T. W.; Weber, R. J., Contribution of water-soluble and insoluble components and their hydrophobic/hydrophilic subfractions to the reactive oxygen species-generating potential of fine ambient aerosols. *Environmental science & technology* **2012,** *46* (20), 11384-11392.
59. Dilger, M.; Orasche, J.; Zimmermann, R.; Paur, H.-R.; Diabaté, S.; Weiss, C., Toxicity of wood smoke particles in human A549 lung epithelial cells: the role of PAHs, soot and zinc. *Archives of toxicology* **2016,** *90* (12), 3029-3044.
60. Lim, C. Y.; Hagan, D. H.; Coggon, M. M.; Koss, A. R.; Sekimoto, K.; Gouw, J. d.; Warneke, C.; Cappa, C. D.; Kroll, J. H., Secondary organic aerosol formation from the laboratory oxidation of biomass burning emissions. *Atmospheric Chemistry and Physics* **2019,** *19* (19), 12797-12809.
61. Karanasiou, A.; Minguillón, M. C.; Viana, M.; Alastuey, A.; Putaud, J.-P.; Maenhaut, W.; Panteliadis, P.; Močnik, G.; Favez, O.; Kuhlbusch, T. A., Thermal-optical analysis for the measurement of elemental carbon (EC) and organic carbon (OC) in ambient air a literature review. **2015**.
62. Tolić, N.; Liu, Y.; Liyu, A.; Shen, Y.; Tfaily, M. M.; Kujawinski, E. B.; Longnecker, K.; Kuo, L.-J.; Robinson, E. W.; Paša-Tolić, L., Formularity: software for automated formula assignment of natural and other organic matter from ultrahigh-resolution mass spectra. *Analytical chemistry* **2017,** *89* (23), 12659-12665.
63. Kujawinski, E. B.; Behn, M. D., Automated analysis of electrospray ionization Fourier transform ion cyclotron resonance mass spectra of natural organic matter. *Analytical chemistry* **2006,** *78* (13), 4363-4373.
64. Hieu, N. T.; Lee, B.-K., Characteristics of particulate matter and metals in the ambient air from a residential area in the largest industrial city in Korea. *Atmospheric Research* **2010,** *98* (2-4), 526-537.
65. Massey, D. D.; Kulshrestha, A.; Taneja, A., Particulate matter concentrations and their related metal toxicity in rural residential environment of semi-arid region of India. *Atmospheric Environment* **2013,** *67*, 278-286.
66. Yuan, Y.; Wu, Y.; Ge, X.; Nie, D.; Wang, M.; Zhou, H.; Chen, M., In vitro toxicity evaluation of heavy metals in urban air particulate matter on human lung epithelial cells. *Science of The Total Environment* **2019,** *678*, 301-308.
67. USEPA, E., Method 3052: Microwave assisted acid digestion of siliceous and organically based matrices. *United States Environmental Protection Agency, Washington, DC USA* **1996**.
68. Creed, J.; Brockhoff, C.; Martin, T., EPA Method 200.8: Determination of Trace Elements in Waters and Wastes by Inductively Coupled Plasma-Mass Spectrometry (Revision 5.4). Cincinnati, OH: United States Environmental Protection Agency (USEPA): 1994.
69. Atwi, K.; Mondal, A.; Pant, J.; Cheng, Z.; El Hajj, O.; Ijeli, I.; Handa, H.; Saleh, R., Physicochemical properties and cytotoxicity of brown carbon produced under different combustion conditions. *Atmospheric Environment* **2021,** *244*, 117881.

70. Groothuis, F. A.; Heringa, M. B.; Nicol, B.; Hermens, J. L.; Blaauboer, B. J.; Kramer, N. I., Dose metric considerations in in vitro assays to improve quantitative in vitro–in vivo dose extrapolations. *Toxicology* **2015,** *332*, 30-40.

71. Doskey, C. M.; van 't Erve, T. J.; Wagner, B. A.; Buettner, G. R., Moles of a substance per cell is a highly informative dosing metric in cell culture. *PloS one* **2015,** *10* (7), e0132572.

72. Bian, Q.; Jathar, S. H.; Kodros, J. K.; Barsanti, K. C.; Hatch, L. E.; May, A. A.; Kreidenweis, S. M.; Pierce, J. R., Secondary organic aerosol formation in biomass-burning plumes: theoretical analysis of lab studies and ambient plumes. *Atmospheric Chemistry and Physics* **2017,** *17* (8), 5459-5475.

73. Roberts, J. M.; Stockwell, C. E.; Yokelson, R. J.; De Gouw, J.; Liu, Y.; Selimovic, V.; Koss, A. R.; Sekimoto, K.; Coggon, M. M.; Yuan, B., The nitrogen budget of laboratory-simulated western US wildfires during the FIREX 2016 Fire Lab study. *Atmospheric Chemistry and Physics* **2020,** *20* (14), 8807-8826.

74. Robinson, M. A.; Decker, Z. C.; Barsanti, K. C.; Coggon, M. M.; Flocke, F. M.; Franchin, A.; Fredrickson, C. D.; Gilman, J. B.; Gkatzelis, G. I.; Holmes, C. D., Variability and Time of Day Dependence of Ozone Photochemistry in Western Wildfire Plumes. *Environmental Science & Technology* **2021,** *55* (15), 10280-10290.

75. Fraser, M. P.; Lakshmanan, K., Using levoglucosan as a molecular marker for the long-range transport of biomass combustion aerosols. *Environmental Science & Technology* **2000,** *34* (21), 4560-4564.

76. Robinson, A. L.; Subramanian, R.; Donahue, N. M.; Bernardo-Bricker, A.; Rogge, W. F., Source apportionment of molecular markers and organic aerosol. 2. Biomass smoke. *Environmental science & technology* **2006,** *40* (24), 7811-7819.

77. de Oliveira Alves, N.; Brito, J.; Caumo, S.; Arana, A.; de Souza Hacon, S.; Artaxo, P.; Hillamo, R.; Teinilä, K.; de Medeiros, S. R. B.; de Castro Vasconcellos, P., Biomass burning in the Amazon region: Aerosol source apportionment and associated health risk assessment. *Atmospheric Environment* **2015,** *120*, 277-285.

78. Medeiros, P. M.; Conte, M. H.; Weber, J. C.; Simoneit, B. R., Sugars as source indicators of biogenic organic carbon in aerosols collected above the Howland Experimental Forest, Maine. *Atmospheric Environment* **2006,** *40* (9), 1694-1705.

79. Kourtchev, I.; Warnke, J.; Maenhaut, W.; Hoffmann, T.; Claeys, M., Polar organic marker compounds in PM2. 5 aerosol from a mixed forest site in western Germany. *Chemosphere* **2008,** *73* (8), 1308-1314.

80. Straka, P.; Havelcova, M., Polycyclic aromatic hydrocarbons and other organic compounds in ashes from biomass combustion. *Acta Geodyn. Geomater* **2012,** *9* (4), 481-490.

81. Smith, J. S.; Laskin, A.; Laskin, J., Molecular characterization of biomass burning aerosols using high-resolution mass spectrometry. *Analytical chemistry* **2009,** *81* (4), 1512-1521.

82. Ghislain, T.; Faure, P.; Michels, R., Detection and monitoring of PAH and Oxy-PAHs by high resolution mass spectrometry: comparison of ESI, APCI and APPI source detection. *Journal of the American Society for Mass Spectrometry* **2012,** *23* (3), 530-536.

83. Aiken, A. C.; Decarlo, P. F.; Kroll, J. H.; Worsnop, D. R.; Huffman, J. A.; Docherty, K. S.; Ulbrich, I. M.; Mohr, C.; Kimmel, J. R.; Sueper, D., O/C and OM/OC ratios of primary, secondary, and ambient organic aerosols with high-resolution time-of-flight aerosol mass spectrometry. *Environmental science & technology* **2008,** *42* (12), 4478-4485.

84. Koch, B. P.; Dittmar, T., From mass to structure: An aromaticity index for high-resolution mass data of natural organic matter. *Rapid communications in mass spectrometry* **2006,** *20* (5), 926-932.

85. Koch, B. P.; Dittmar, T., From mass to structure: an aromaticity index for high-resolution mass data of natural organic matter. *Rapid Communications in Mass Spectrometry* **2016,** *30* (1), 250-250.

86. Willoughby, A. S.; Wozniak, A. S.; Hatcher, P. G., Detailed source-specific molecular composition of ambient aerosol organic matter using ultrahigh resolution mass spectrometry and 1H NMR. *Atmosphere* **2016,** *7* (6), 79.

87. Wang, Y.; Hu, M.; Lin, P.; Tan, T.; Li, M.; Xu, N.; Zheng, J.; Du, Z.; Qin, Y.; Wu, Y., Enhancement in particulate organic nitrogen and light absorption of humic-like substances over Tibetan Plateau due to long-range transported biomass burning emissions. *Environmental science & technology* **2019,** *53* (24), 14222-14232.
88. Kay, J. G.; Grinstein, S., Sensing phosphatidylserine in cellular membranes. *Sensors* **2011,** *11* (2), 1744-1755.
89. Wlodkowic, D.; Telford, W.; Skommer, J.; Darzynkiewicz, Z., Apoptosis and beyond: cytometry in studies of programmed cell death. *Methods in cell biology* **2011,** *103*, 55-98.
90. Berghe, T. V.; Linkermann, A.; Jouan-Lanhouet, S.; Walczak, H.; Vandenabeele, P., Regulated necrosis: the expanding network of non-apoptotic cell death pathways. *Nature reviews Molecular cell biology* **2014,** *15* (2), 135-147.
91. Gary, A.-S.; Rochette, P. J., Apoptosis, the only cell death pathway that can be measured in human diploid dermal fibroblasts following lethal UVB irradiation. *Scientific reports* **2020,** *10* (1), 1-11.
92. Quezada-Maldonado, E. M.; Sánchez-Pérez, Y.; Chirino, Y. I.; García-Cuellar, C. M., Airborne Particulate Matter induces oxidative damage, DNA adduct formation and alterations in DNA repair pathways. *Environmental Pollution* **2021**, 117313.
93. Huang, C.-T.; Huang, D.-Y.; Hu, C.-J.; Wu, D.; Lin, W.-W., Energy adaptive response during parthanatos is enhanced by PD98059 and involves mitochondrial function but not autophagy induction. *Biochimica et Biophysica Acta (BBA)-Molecular Cell Research* **2014,** *1843* (3), 531-543.
94. Lin, P.; Bluvshtein, N.; Rudich, Y.; Nizkorodov, S. A.; Laskin, J.; Laskin, A., Molecular chemistry of atmospheric brown carbon inferred from a nationwide biomass burning event. *Environmental science & technology* **2017,** *51* (20), 11561-11570.
95. Lovera-Leroux, M.; Crobeddu, B.; Kassis, N.; Petit, P. X.; Janel, N.; Baeza-Squiban, A.; Andreau, K., The iron component of particulate matter is antiapoptotic: A clue to the development of lung cancer after exposure to atmospheric pollutants? *Biochimie* **2015,** *118*, 195-206.
96. Chen, L. C.; Lippmann, M., Effects of metals within ambient air particulate matter (PM) on human health. *Inhalation toxicology* **2009,** *21* (1), 1-31.
97. Zhao, H.; Cui, B.; Zhang, K., The distribution of heavy metal in surface soils and their uptake by plants along roadside slopes in longitudinal range gorge region, China. *Environmental Earth Sciences* **2010,** *61* (5), 1013-1023.
98. Qiao, P.; Yang, S.; Lei, M.; Chen, T.; Dong, N., Quantitative analysis of the factors influencing spatial distribution of soil heavy metals based on geographical detector. *Science of the Total Environment* **2019,** *664*, 392-413.
99. Yang, A.; Jedynska, A.; Hellack, B.; Kooter, I.; Hoek, G.; Brunekreef, B.; Kuhlbusch, T. A.; Cassee, F. R.; Janssen, N. A., Measurement of the oxidative potential of PM2. 5 and its constituents: The effect of extraction solvent and filter type. *Atmospheric Environment* **2014,** *83*, 35-42.
100. Verma, V.; Rico-Martinez, R.; Kotra, N.; Rennolds, C.; Liu, J.; Snell, T. W.; Weber, R. J., Estimating the toxicity of ambient fine aerosols using freshwater rotifer Brachionus calyciflorus (Rotifera: Monogononta). *Environmental pollution* **2013,** *182*, 379-384.
101. Rahman, Z.; Singh, V. P., The relative impact of toxic heavy metals (THMs)(arsenic (As), cadmium (Cd), chromium (Cr)(VI), mercury (Hg), and lead (Pb)) on the total environment: an overview. *Environmental monitoring and assessment* **2019,** *191* (7), 1-21.
102. Osorio-Rico, L.; Santamaria, A.; Galván-Arzate, S., Thallium toxicity: general issues, neurological symptoms, and neurotoxic mechanisms. *Neurotoxicity of Metals* **2017**, 345-353.
103. Jomova, K.; Baros, S.; Valko, M., Redox active metal-induced oxidative stress in biological systems. *Transition Metal Chemistry* **2012,** *37* (2), 127-134.

709 104. Dashner-Titus, E. J.; Schilz, J. R.; Simmons, K. A.; Duncan, T. R.; Alvarez, S. C.; Hudson, L. G.,
710 Differential response of human T-lymphocytes to arsenic and uranium. *Toxicology Letters* **2020,** *333*, 269-
711 278.
712 105. Luo, T.; Yuan, Y.; Yu, Q.; Liu, G.; Long, M.; Zhang, K.; Bian, J.; Gu, J.; Zou, H.; Wang, Y., PARP-1
713 overexpression contributes to Cadmium-induced death in rat proximal tubular cells via parthanatos and
714 the MAPK signalling pathway. *Scientific reports* **2017,** *7* (1), 1-13.
715 106. Liu, L.; Urch, B.; Szyszkowicz, M.; Evans, G.; Speck, M.; Van Huang, A.; Leingartner, K.; Shutt,
716 R. H.; Pelletier, G.; Gold, D. R., Metals and oxidative potential in urban particulate matter influence
717 systemic inflammatory and neural biomarkers: A controlled exposure study. *Environment international*
718 **2018,** *121*, 1331-1340.
719 107. Pardo, M.; Qiu, X.; Zimmermann, R.; Rudich, Y., Particulate matter toxicity is nrf2 and
720 mitochondria dependent: The roles of metals and polycyclic aromatic hydrocarbons. *Chemical research in*
721 *toxicology* **2020,** *33* (5), 1110-1120.
722 108. Leclercq, B.; Kluza, J.; Antherieu, S.; Sotty, J.; Alleman, L. Y.; Perdrix, E.; Loyens, A.; Coddeville,
723 P.; Guidice, J.-M. L.; Marchetti, P.; Garçon, G., Air pollution-derived PM2.5 impairs mitochondrial function
724 in healthy and chronic obstructive pulmonary diseased human bronchial epithelial cells. *Environmental*
725 *pollution* **2018,** *243*, 1434-1449.
726 109. Chew, S.; Lampinen, R.; Saveleva, L.; Korhonen, P.; Mikhailov, N.; Grubman, A.; Polo, J. M.;
727 Wilson, T.; Komppula, M.; Rönkkö, T., Urban air particulate matter induces mitochondrial dysfunction in
728 human olfactory mucosal cells. *Particle and fibre toxicology* **2020,** *17*, 1-15.
729 110. Sharma, J.; Parsai, K.; Raghuwanshi, P.; Ali, S. A.; Tiwari, V.; Bhargava, A.; Mishra, P. K., Emerging
730 role of mitochondria in airborne particulate matter-induced immunotoxicity. *Environmental Pollution*
731 **2020**, 116242.
732 111. Jiang, Q.; Ji, A.; Li, D.; Shi, L.; Gao, M.; Lv, N.; Zhang, Y.; Zhang, R.; Chen, R.; Chen, W.,
733 Mitochondria damage in ambient particulate matter induced cardiotoxicity: Roles of PPAR alpha/PGC-1
734 alpha signaling. *Environmental Pollution* **2021**, 117792.

735